

ESR Spectra of Low-Symmetry High-Spin Cobalt(II) Complexes. 2. Pseudotetrahedral Dichlorobis(triphenylphosphine oxide)cobalt(II)¹

A. BENCINI, C. BENELLI, D. GATTESCHI,* and C. ZANCHINI

Received January 5, 1979

The single-crystal ESR and polarized electronic spectra of bis(triphenylphosphine oxide)cobalt(II) dichloride have been recorded. The effective g values have been found to be highly anisotropic, with $g_1 = 5.67$, $g_2 = 3.59$, and $g_3 = 2.16$. For the interpretation of these data a completely symmetry-independent ligand field approach to the energies of the electronic levels and to the low-symmetry g tensor has been used. The results have been most satisfactory since the model accounted easily for the high observed anisotropy of the g values. It is proposed that by this model it is possible to rationalize the ESR spectra of low-symmetry high-spin cobalt(II) complexes.

Introduction

Although ESR spectroscopy has been much used for the characterization of transition-metal complexes, the studies of high-spin cobalt(II) complexes are still relatively scarce.^{2,3} Since the call for spectral information on cobalt(II) complexes has increased greatly in the last few years, principally due to the impact of bioinorganic chemistry, where cobalt can often substitute zinc in metalloenzymes maintaining the biological activity,⁴ we decided to attempt a thorough characterization of ESR spectra of high-spin cobalt(II).

Beyond the experimental difficulties, due to the necessity to obtain very low temperatures in order to have reasonably narrow signals, many problems arise in the interpretation of the spectra since low-symmetry components play a major role in determining the resonance fields. As a matter of fact it is now apparent that seemingly symmetric configurations of ligands can yield highly anisotropic g values.^{1,5-10} It is now clear, therefore, that idealized symmetries, which were of great help in the interpretation of the electronic spectra, are of little use for the interpretation of ESR and magnetic properties. By use of the spin Hamiltonian formalism, five parameters are needed (g_x , g_y , g_z , D , and E), and because only a transition between one Kramers doublet is observed, which yields three experimental data, the interpretation of the spectra is not unambiguous. Further, the values of the g and D tensors by themselves have only a bookkeeping meaning, and they must be checked against some theoretical calculation in order to relate them to the electronic structure of the complex.

In the last few years the extension of the ligand field formalism to low-symmetry complexes has appeared to be useful,¹¹⁻¹⁹ especially resorting to the angular-overlap model. According to this scheme it is possible in principle to transfer the values of e_λ parameters of a ligand from one complex to another provided that some caution is exerted.²⁰ By this method it was possible to consider series of complexes and to calculate reasonable sets of parameters which fit the electronic transitions. Recently Gerloch et al.²¹ suggested a method for calculating the anisotropic magnetic susceptibilities of low-symmetry complexes, without making any use of idealized symmetries, and applied it with success to several complexes.²²⁻²⁴ It appeared to us that such a model might be of great help in the interpretation of the ESR spectra of high-spin cobalt(II), giving the full theoretical information to be compared with the experimental data. Therefore, we resorted to a study of some low-symmetry cobalt(II) complexes in order to see how this approach could be of help and to develop the model more fully for an ESR spectroscopist.

For this purpose we choose the complex dichlorobis(triphenylphosphine oxide)cobalt(II), $\text{CoCl}_2(\text{Ph}_3\text{PO})_2$, which can be doped into the zinc analogue which is known to be pseudotetrahedral with a C_2 site symmetry.²⁵ C_2 symmetry implies that one direction of the g and A tensors is fixed, while the

other two are to be determined. This gives us the required low symmetry, but with the obvious simplification of only two principal directions to be determined. We wish to report here the single-crystal ESR and electronic spectra of $\text{CoCl}_2(\text{Ph}_3\text{PO})_2$, together with their interpretation based on the angular overlap model.

Experimental Section

$\text{CoCl}_2(\text{Ph}_3\text{PO})_2$ and $\text{ZnCl}_2(\text{Ph}_3\text{PO})_2$ were prepared as previously described.²⁶ Single crystals of cobalt(II) doped into $\text{ZnCl}_2(\text{Ph}_3\text{PO})_2$ were grown by slow evaporation of methylene chloride and *n*-butyl ether solutions. The crystals were oriented by Weissenberg techniques and were found to be isostructural to the copper analogue.²⁷ The shape of the crystals is that of prisms with the (110) face highly developed and c as the long axis.

The single-crystal polarized electronic spectra were recorded with a Cary 17 spectrophotometer equipped with an Oxford Instruments liquid helium continuous-flow cryostat. ESR spectra were recorded with a Varian E-9 spectrometer operating at 9 GHz and equipped with Oxford Instruments ESR 9 continuous-flow cryostat. The crystals were mounted on a Perspex rod by using the geometrical features for the orientation.

Results

ESR Spectra. The polycrystalline powder ESR spectra of $(\text{Co,Zn})\text{Cl}_2(\text{Ph}_3\text{PO})_2$ recorded at 4.2 K are shown in Figure 1. The bandwidths are dramatically temperature dependent. The shape of the lowest field feature seems to be due to unresolved hyperfine interaction. The g values (according to a Hamiltonian with an effective spin of $S = 1/2$) are $g_1 = 5.7 \pm 0.2$, $g_2 = 3.59 \pm 0.05$, and $g_3 = 2.16 \pm 0.04$. The powder spectra of the pure cobalt complex are practically identical to those of the zinc-doped complex.

The single-crystal spectra confirm that the three features seen in the powder spectra are associated with the same transition. Since the metal ions have C_2 site symmetry in the lattice, a principal direction of g is individuated by the c crystal axis. The corresponding g value was found to be $g_2 = 3.59 \pm 0.02$.

The signal shows evidence of unresolved hyperfine splitting within a Gaussian line shape; $|A_2|$ can be estimated as $<6 \times 10^{-4} \text{ cm}^{-1}$.

Spectra recorded with the static magnetic field in the (001) plane showed the presence of two magnetically nonequivalent sites, in accord with the orthorhombic symmetry of the lattice. The angular dependence of the observed g^2 values is shown in Figure 2. The principal g_3 values were found at $\pm 30 \pm 5^\circ$ from a , with $g_3 = 2.16 \pm 0.02$, and correspondingly, the g_1 values were found at $\pm 30 \pm 5^\circ$ from b , with $g_1 = 5.67 \pm 0.03$. Along this direction a hyperfine splitting into eight lines due to the coupling of the unpaired electrons with ^{59}Co was observed, with $|A_1| = 53 \pm 6 \times 10^{-4} \text{ cm}^{-1}$. By rotation of the crystal away from this direction, the hyperfine splitting becomes smaller, until it is no longer resolved. From the line

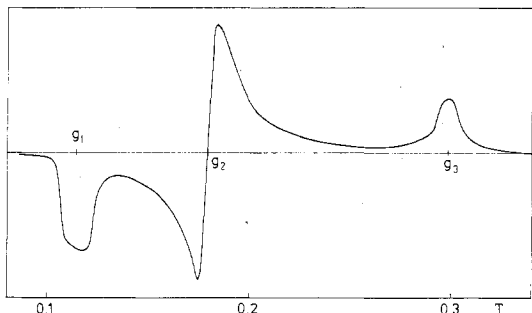


Figure 1. Polycrystalline powder ESR spectra of $(\text{Co,Zn})\text{Cl}_2(\text{Ph}_3\text{PO})_2$ recorded at X-band frequency at 4.2 K.

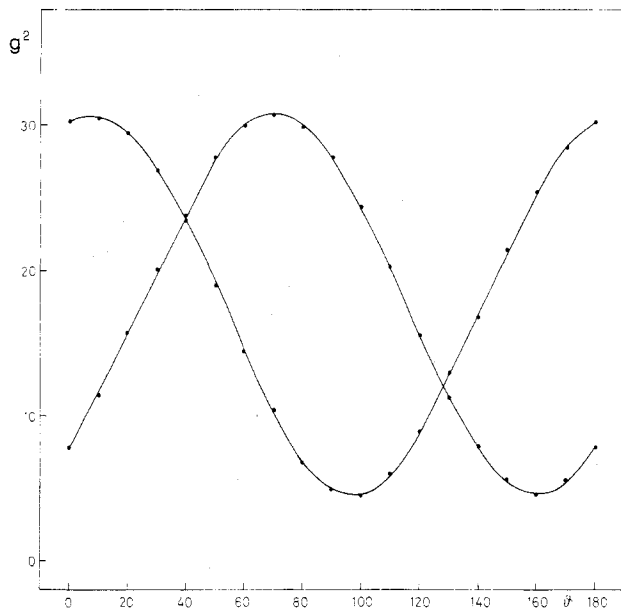


Figure 2. Angular dependence of the g^2 values in the (001) plane. The curve corresponds to the least-squares fit of the experimental points. For $\theta = 0^\circ$ the static magnetic field is parallel to $\{110\}$.

shape, $|A_3|$ can be estimated as $<6 \times 10^{-4} \text{ cm}^{-1}$.

Electronic Spectra. The single-crystal polarized electronic spectra were recorded on the highly developed (110) face, with the electric vector of the incident radiation parallel to c and to $\{110\}$, respectively. The spectra, recorded at 4.2 K, are shown in Figure 3. They show the effect of stray light, presumably due to the poor quality of the crystal.

A band at $\sim 5 \times 10^3 \text{ cm}^{-1}$ is more intense parallel to c , while a band at $6.8 \times 10^3 \text{ cm}^{-1}$ is in every case of low intensity. The high-frequency band shows at least two maxima at 15 and $16.7 \times 10^3 \text{ cm}^{-1}$. The former does not show any distinct polarization properties, while the latter is more intense parallel to $\{110\}$. The maxima seen at $\sim 13000 \text{ cm}^{-1}$ do not correspond to any transition seen in the diffuse reflectance spectra at room temperature and might be due to stray-light effects or to spin-forbidden transitions.

Discussion

The ESR spectra of $(\text{Co,Zn})\text{Cl}_2(\text{Ph}_3\text{PO})_2$ can be interpreted as being due to the $\pm 1/2$ transition on the basis of the angular dependence. By use of a completely anisotropic spin Hamiltonian with effective spin $S = 1/2$, five independent parameters must be determined by the reported expressions,^{23-26,28} namely, g_x , g_y , g_z , D , and E . Since this number exceeds the number of experimentally available transitions, some assumptions must be made.

If it is assumed that $g_x = g_y = g_{\perp}$, it is found that the spectra can be fit with the values $g_{\parallel} = 2.31$, $g_{\perp} = 2.35$, and $E/D =$

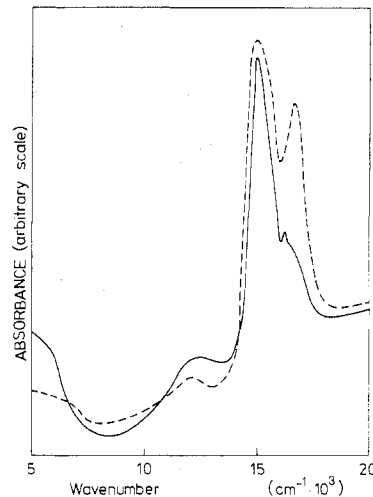


Figure 3. Single-crystal polarized electronic spectra in the (110) plane of $(\text{Co,Zn})\text{Cl}_2(\text{Ph}_3\text{PO})_2$: —, electric vector parallel to $\{001\}$; ---, electric vector parallel to $\{110\}$.

-0.152 . These parameters are independent of D , provided that D is larger than 3 cm^{-1} . Although these results can be considered with some confidence, it is evident that more information would be welcome for a satisfactory interpretation of the data. Further, a model is required which can give physical meaning to these parameters.

Recently Gerloch²¹ suggested a general model for the calculation of the energies of the electronic transitions and of the magnetic properties of low-symmetry complexes. In this approach he does not assume any idealized symmetry and calculates both the principal values and directions of the tensors which are relevant to the interpretation of the magnetic properties of the complexes. In order to interpret our ESR data, his treatment of the g^2 tensor is important. It assumes the presence of isolated multiplets and, given a laboratory axis frame, calculates a nondiagonal g^2 tensor, according to the relation

$$g^2_{\alpha\beta} = n \sum_i \sum_k \langle i | \mu_{\alpha} | k \rangle \langle k | \mu_{\beta} | i \rangle \quad (1)$$

where α and β are arbitrary Cartesian components, μ_{α} and μ_{β} are the α th and β th components of the Zeeman operator, the sums are over all the functions which are degenerate in the absence of a magnetic field, and n is a number which depends on the degeneracy of the multiplet in the absence of magnetic field. The energy levels in the absence of the field are computed through a ligand field spin-orbit coupling treatment, either in the classic crystal field or in the angular-overlap formalism.

In the case of the low-symmetry cobalt(II) complexes, the energy levels will be degenerate in pairs. The separation between the two lowest energy levels gives the zero-field splitting $2(D^2 + 3E^2)^{1/2}$ while the g values calculated for the various Kramers doublets can be directly compared to the g values of the $S = 1/2$ effective spin Hamiltonian.

In our calculations we use a basis of 40 functions corresponding to the quartet states.

In order to apply the model to the present compound, it is necessary to make a choice of angular coordinates. The crystal structure of $\text{ZnCl}_2(\text{Ph}_3\text{PO})_2$ has not been reported, although it was shown to be isomorphous to the copper(II) analogue,²⁷ space group $Fdd2$. Also, the structure of $\text{CoCl}_2(\text{Ph}_3\text{PO})_2$ has been reported,²⁹ the space group being monoclinic Cc .

Since the ESR spectra of the undiluted cobalt(II) complex are practically identical with those of the zinc doped, we used the latter coordinates for the assignments of the spectra. However, the cell dimensions are surprisingly similar to those

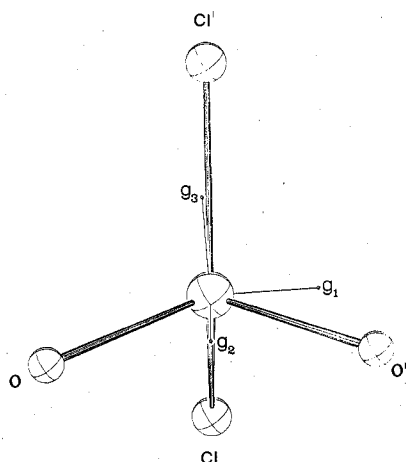


Figure 4. The orientation of the principal axes of g within the molecular frame.

of the orthorhombic complexes. As a matter of fact, if reduced cell arguments³⁰ are used, it is found that the monoclinic cell is related to the orthorhombic one by the transformation

$$\begin{pmatrix} -1 & 0 & -2 \\ 0 & 1 & 0 \\ -1 & 0 & 0 \end{pmatrix}$$

Therefore, we decided to use the reported coordinates²⁹ to calculate not only the molecular g values but also their orientations in the crystal. In Figure 4 the orientation of the principal g axes within the molecular frame is shown. Since the lattice of the zinc host is orthorhombic, there are two possible choices, which lead to two sets of g axes, rotated by 60° along c . According to one choice, the two g values are close to the projections of the Co-Cl and Co-O bonds on the plane perpendicular to C_2 . The other choice sets the g values close to the bisectors of the Cl-M-O angles. In Figure 4 we have conformed to the former, for reasons which will become clear below.

The program requires the e_λ parameters of the ligands as an input, as well as the spin-orbit coupling constant ζ_i and the orbital reduction factor³¹ k_i (i indicates a Cartesian component). In order to keep the number of parameters to a minimum, both k and ζ were considered as isotropic. The e_σ and e_π parameters of the chlorine atoms were fixed at the values reported by Horrocks³² for CoCl_4^{2-} . The other e_λ parameters were allowed to vary, together with k and ζ , while keeping the geometrical factors constant. The results of some representative calculations of the g values are shown in Figure 5. The variations shown correspond to a $Dq = (1/10)[3e_\sigma - 4e_\pi]$ range for the phosphine oxide ligand of $800\text{--}1000\text{ cm}^{-1}$, which seems to be appropriate for the energies of the electronic transitions.

The e_π^O/e_σ^O ratio is seen to affect the calculated g values, and so does also the $e_{\pi c}^O/e_{\pi s}^O$ ratio. If we proceed as was suggested for the pyridine N -oxide complexes,³⁷ the $e_{\pi c}^O/e_{\pi s}^O$ ratio can be shown to vary between 0.67 and 1.00 for sp^2 - and sp -hybridized oxygen. Since in the present case the Co-O-P angle is 150° , the ratio is expected to be somewhere between the two limits. The values of the parameters which were found to give satisfactory agreement with the ESR and optical data fixing $e_{\pi c}^O/e_{\pi s}^O = 1$ are $e_\sigma^O = 5400\text{--}6100\text{ cm}^{-1}$, $e_\pi^O/e_\sigma^O = 0.3\text{--}0.4$, and $k = 0.85\text{--}0.90$, with ζ at the free-ion value.³⁸ Relaxing the $e_{\pi c}^O/e_{\pi s}^O$ ratio slightly, one finds different fits, with no significant improvement. For instance fixing $e_{\pi c}^O/e_{\pi s}^O = 0.8$, one can obtain fits with the following parameters: $e_\sigma^O = 4700\text{--}5050\text{ cm}^{-1}$, $e_{\pi s}^O/e_\sigma^O = 0.3\text{--}0.4$, and $k = 0.85\text{--}0.90$, with ζ at the free-ion value. It is worth mentioning that with these values the principal directions are also nicely reproduced,

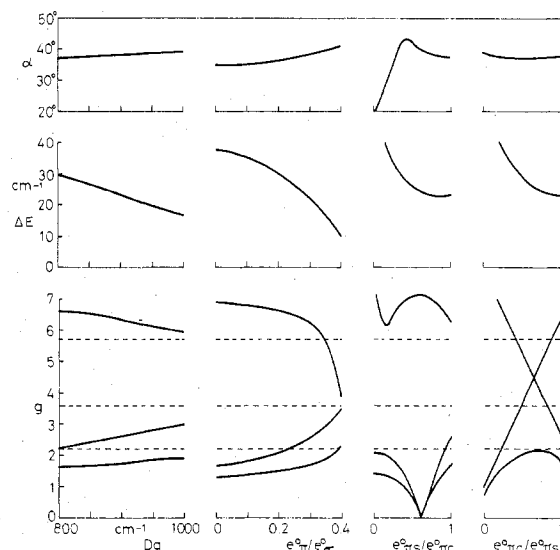


Figure 5. The dependence of g , the zero-field splitting ΔE , and the angle of g_3 to the a axis, α , on the ligand field parameters. On the left is the variation of Dq for the oxygen donors with $e_{\text{Cl}}^{\text{Cl}} = 5700\text{ cm}^{-1}$, $e_{\pi}^{\text{Cl}} = 2400\text{ cm}^{-1}$, $e_{\pi}^{\text{O}}/e_{\sigma}^{\text{O}} = 0.3$, $\zeta = 533\text{ cm}^{-1}$, $k = 0.9$, and $B = 800\text{ cm}^{-1}$. From left to right is shown the effect of changing the parameters at the bottom in turn, leaving all the others unchanged. The Dq value in these diagrams is 900 cm^{-1} .

Table I. Representative Fit of the Principal g Values and Directions (Parameter Values: $B = 730$, $e_{\text{Cl}}^{\text{Cl}} = 5700$, $e_{\pi}^{\text{Cl}} = 2400$, $e_{\sigma}^{\text{O}} = 4750$, $e_{\pi s}^{\text{O}} = 1945$, $e_{\pi c}^{\text{O}} = 1555$, $\zeta = 533\text{ cm}^{-1}$, $k = 0.9$)

	g values		α^a	
	calcd	obsd	calcd	obsd
g_1	5.68	5.67 ± 0.03	127	120 ± 5
g_2	3.68	3.59 ± 0.02		
g_3	2.07	2.16 ± 0.02	37	30 ± 5

α^a is the angle between the indicated g direction and the a crystal axis in the ab plane.

with the smallest g value which makes an angle of $30\text{--}40^\circ$ to the a axis and the intermediate g value parallel to c . This corresponds to setting g_1 close to the bond projections. No fit could be found if the g_1 and g_3 experimental values were considered to bisect the Cl-M-O angles. A typical fitting of the g values and directions is shown in Table I. The calculated energies of the electronic transitions were all within 1500 cm^{-1} from the observed transitions.

Conclusions

The ligand field model has been shown to be an invaluable tool for the interpretation of the spectral and magnetic properties of low-symmetry high-spin cobalt(II) complexes. In particular, with values of the parameters which compare well with previous spectroscopic data, it can give a very effective means of rationalization of the highly anisotropic g factors which are often found for high-spin cobalt(II) complexes. The purpose of this kind of analysis should be that of making ESR a tool for the diagnosis of subtle structural differences in various complexes. Whether this will be possible or not cannot be said now, but it is important that a simple theoretical model is made available to the spectroscopist.

Acknowledgment. Thanks are due to Professor L. Sacconi for encouragement.

Registry No. $\text{CoCl}_2(\text{Ph}_3\text{PO})_2$, 14494-82-7; $\text{ZnCl}_2(\text{Ph}_3\text{PO})_2$, 14494-88-3.

References and Notes

- (1) Part I: Bencini, A.; Gatteschi, D. *Inorg. Chem.* **1977**, *16*, 2141.
- (2) McGarvey, B. R. *Transition Met. Chem.* **1966**, *3*, 90.

- (3) Goodman, P. A.; Raynor, J. B. *Adv. Inorg. Chem. Radiochem.* **1970**, *13*, 135.
 (4) Ulmer, D. D.; Vallee, B. L. *Adv. Chem. Ser.* **1971**, No. 100.
 (5) Yamaka, E.; Barnes, R. G. *Phys. Rev.* **1962**, *125*, 1568.
 (6) Gladney, H. M. *Phys. Rev.* **1966**, *143*, 198.
 (7) Carlin, R. L.; O'Connor, C. J.; Bathia, S. N. *J. Am. Chem. Soc.* **1976**, *98*, 685.
 (8) Kennedy, F. S.; Hill, H. A. O.; Kaden, T. A.; Vallee, B. L. *Biochem. Biophys. Res. Commun.* **1972**, *48*, 1533.
 (9) Yablokov, Yu. V.; Voronkova, V. K.; Shishkov, V. F.; Ablov, A. V.; Vaishein, Zh. Yu. *Sov. Phys.-Solid State (Engl. Transl.)* **1972**, *13*, 831.
 (10) Guggenberger, L. J.; Prewitt, C. T.; Meakin, P.; Trofimenko, S.; Jesson, J. P. *Inorg. Chem.* **1973**, *12*, 508.
 (11) Hitchman, M. A. *Inorg. Chem.* **1972**, *11*, 2837.
 (12) Ciampolini, M. *Struct. Bonding (Berlin)* **1969**, *6*, 52.
 (13) Lever, A. B. P. *Coord. Chem. Rev.* **1968**, *3*, 119.
 (14) Glerup, J.; Mønsted, O.; Schäffer, C. E. *Inorg. Chem.* **1976**, *15*, 1399.
 (15) Hathaway, B. J.; Tomlinson, A. A. G. *Coord. Chem. Rev.* **1970**, *5*, 1.
 (16) Gerloch, M.; Kohl, J.; Lewis, J.; Umland, W. *J. Chem. Soc. A* **1970**, 3283.
 (17) Bertini, I.; Gatteschi, D.; Scozzafava, A. *Isr. J. Chem.* **1976**, *15*, 189.
 (18) Schreiner, A. F.; Hamm, D. J. *Inorg. Chem.* **1973**, *12*, 2041.
 (19) Smith, D. W. *Struct. Bonding (Berlin)* **1972**, *12*, 149.
 (20) Schäffer, C. E. "Wave Mechanics"; Butterworths: London, 1973.
 (21) Gerloch, M.; McMeeking, R. F. *J. Chem. Soc., Dalton Trans.* **1975**, 2443.
 (22) Gerloch, M.; McMeeking, R. F.; White, M. A. *J. Chem. Soc., Dalton Trans.* **1976**, 655.
 (23) Gerloch, M.; Cruse, D. A. *J. Chem. Soc., Dalton Trans.* **1977**, 152.
 (24) Gerloch, M.; Cruse, D. A. *J. Chem. Soc., Dalton Trans.* **1977**, 1613.
 (25) Vivien, D.; Gibson, J. F. *J. Chem. Soc., Faraday Trans. 2* **1975**, *71*, 1640.
 (26) Goodgame, D. M. L.; Cotton, F. A. *J. Chem. Soc. A* **1969**, 2298.
 (27) Bertrand, J. A.; Kalyanaraman, A. R. *Inorg. Chim. Acta* **1971**, *5*, 341.
 (28) Pilbrow, J. R. *J. Magn. Reson.* **1978**, *31*, 479.
 (29) Mangion, M. M.; Smith, R.; Shore, S. G. *Cryst. Struct. Commun.* **1976**, *5*, 49.
 (30) Lawton, S. L.; Jacobson, R. A. "The Reduced Cell and Its Crystallographic Applications", Research and Development Report; AEC: 1965.
 (31) Stevens, K. W. M. *Proc. R. Soc. London, Ser. A* **1953**, *219*, 542.
 (32) Horrocks, W. De W.; Burlone, D. A. *J. Am. Chem. Soc.* **1976**, *98*, 6512.
 (33) Carlin, R. L.; O'Connor, C. J.; Bathia, S. N. *J. Am. Chem. Soc.* **1976**, *98*, 3523.
 (34) Van Ingen Schenau, A. D.; Verschoor, G. C.; Romers, C. *Acta Crystallogr.* **1974**, *330*, 1686.
 (35) Bugendahl, T. J.; Wood, J. S. *Inorg. Chem.* **1975**, *14*, 338.
 (36) Mackey, D. J.; McMeeking, R. F. *J. Chem. Soc., Dalton Trans.* **1977**, 2186.
 (37) Mackey, D. J.; Evans, S. V.; McMeeking, R. F. *J. Chem. Soc., Dalton Trans.* **1978**, 160.
 (38) Griffith, J. S. "The Theory of Transition Metal Ions"; Cambridge University Press: London, 1971.

Contribution from the Physikalisch-chemisches Institut der Universität Basel, CH-4056 Basel, Switzerland

Emission Spectrum of Tri-*B*-fluoroborazine Radical Cation in the Gas Phase: $\tilde{A}^2A_2'' \rightarrow \tilde{X}^2E''$ Band System

TAYLOR B. JONES, JOHN P. MAIER,* and OSKAR MARTHALER

Received December 15, 1978

The optical emission spectrum of the tri-*B*-fluoroborazine radical cation in the gas phase has been obtained. The band system is assigned to the $\tilde{A}^2A_2'' \rightarrow \tilde{X}^2E''$ electronic transition of the cation by reference to the photoelectron spectrum of tri-*B*-fluoroborazine which was recorded under higher resolution. A vibrational analysis of the emission band system yields the frequencies of three of the four A_1' (under D_{3h} symmetry classification) fundamentals for the \tilde{X}^2E'' state whereas the Ne I photoelectron spectrum allows the corresponding three frequencies for the \tilde{A}^2A_2'' state of tri-*B*-fluoroborazine cation to be deduced.

Introduction

Optical emission spectra of polyatomic radical cations in the gas phase have recently been obtained for several groups of organic species.^{1,2} These radical cations range from tetraatomic systems such as the haloacetylenes³ to the 18-atomic octatetraene.⁴ In the case of inorganic radical cations, however, the detection of the radiative relaxation channel has been limited to the triatomic cations N_2O^+ ,⁵ H_2S^+ ,⁶ H_2O^+ ,⁷ and SO_2^+ .⁸ In this work we report the emission spectrum of the first large inorganic radical cation, tri-*B*-fluoroborazine, in its first excited cationic state.

The observation of the emission spectrum allows us to infer the frequencies of three of the four totally symmetric fundamentals (A_1' under D_{3h} classification) for the ground state of the tri-*B*-fluoroborazine radical cation from the analysis of the band system. In addition, the frequencies of these vibrational modes have also been obtained for the first excited cationic state from the photoelectron spectrum of tri-*B*-fluoroborazine which was recorded under high resolution. For the molecular ground state the corresponding frequencies have not been given in the literature as only the bands in the gas-phase IR spectra have hitherto been reported.⁹

Experimental Section

The emission spectrum was measured by using the apparatus and techniques which have been described in an earlier work.³ The spectra shown in Figure 1 were obtained by an electron beam of ~ 40 eV in energy, ~ 450 μA in current, impacting on an effusive sample beam at a pressure of $\sim 10^{-3}$ torr. The emitted radiation was dispersed with an optical resolution of 1.6 nm in the first run and 0.8 nm in the second,

during which the sample was exhausted. The resolution used was dictated by the weakness of the emission. The data were accumulated on-line with a computer and then corrected for the optical transmission function of the apparatus and converted to a wavenumber, cm^{-1} , scale. The sample was introduced into the instrument from a glass vessel held in a bath at room temperature. The sample of tri-*B*-fluoroborazine was prepared according to the procedure given in the literature and purified by vacuum distillation.⁹ The high-resolution photoelectron spectra were obtained with a spectrometer incorporating a $\pi/2^{1/2}$ cylindrical sector analyzer.¹⁰ The resolving power of the instrument was ~ 250 and the spectrum shown in Figure 2 was excited with the Ne I (16.85 eV) photon resonance line in order to resolve more distinctly the low-frequency vibrational fine structure on the lowest ionization energy bands. The energy scale was internally calibrated by using xenon.

Results and Discussion

The emission spectrum which is attributed to the $\tilde{A} \rightarrow \tilde{X}$ electronic transition of the radical cation of tri-*B*-fluoroborazine is shown in Figure 1. The assignment is made on the basis of the photoelectron spectrum of tri-*B*-fluoroborazine^{11,12} which shows that the separation of the first two bands corresponds to the energy region spanned by the emission band system, ~ 1.9 – 2.4 eV. In Figure 2 is reproduced a high resolution Ne I photoelectron spectrum in the region from 10 to 15 eV. The photoelectron spectrum, at lower resolution, has been reported earlier by two groups and an assignment of the bands was proposed.^{11,12} In the case of the ground and first excited electronic state of tri-*B*-fluoroborazine cation the symmetries $^2E''$ and $^2A_2''$, respectively, have been deduced.